Proceedings of the 1999 IEEE
International Conference on Robotics & Automation
Detroit, Michigan • May 1999

Unified Analysis on Mobility and Manipulability of Mobile Manipulators

Yoshio Yamamoto
Dept. of Precision Mechanics
Tokai University
Hiratsuka, Japan 259-1292

Xiaoping Yun
Dept. of Elec. and Comp. Engineering
Naval Postgraduate School
Monterey, CA, 93943-5121

ABSTRACT

This paper presents an unified approach to the task space analysis of a wheeled mobile manipulator interacting with the environment. A system considered in this paper is two articulated manipulators atop a wheeled mobile platform handling a common object. We derive the task space ellipsoid, both kinematic and dynamic, for a wheeled mobile manipulator which takes into account manipulation and locomotion. The ellipsoid is able to visualize how the manipulator and the platform can contribute to a task execution by integrating the mobility of the platform with the manipulability of the arms as one unified measure. This measure can be useful not only for the task space analysis of a single mobile manipulator, but also for the coordination of multiple arms, mobile robots or mobile manipulators.

1 Introduction

In the recent years, there has been a great deal of interest in *mobile manipulators* [1, 5, 10, 11, 12, 13, 14]. A mobile manipulator typically consists of a mobile platform and a robotic manipulator mounted on the platform, which combines the dextrous manipulation capability offered by fixed-base manipulators and the mobility provided by mobile platforms. A mobile manipulator therefore has a considerably larger workspace than a fixed-base one, and has many potential applications in manufacturing, nuclear reactor maintenance, construction, and planetary exploration.

Coordination of manipulation and locomotion is one of the main research topics of mobile manipulators. The majority of the early work on mobile manipulators, however, focuses on the coordination of locomotion and manipulation by considering the manipulator and the platform as two independent entities. Also they do not take interactions with the environment into account. Separating manipulation from mobility makes control and planning problems easier, but it will be much more effective and efficient if the manipulator can execute a given task while the platform is moving. We proposed a coordination algorithm of mobile manipulators which utilizes manipulability measure of the arm [13].

Concept of the manipulability ellipsoid was originally introduced by Yoshikawa [17, 16]. Manipulability has been utilized in many applications such as design and control of redundant manipulators [6], dual-arm cooperation [7, 2], multi-fingered grasping [8], multiple arm systems (more than two arms) [3], and coordination between manipulation and locomotion of a mobile manipulator [13].

Unlike our previous work in which the manipulability of a manipulator was employed for the coordination purpose between the manipulator and the mobile platform, the present work treats both locomotion and manipulation in the same framework from the viewpoint of task space. Contribution of the manipulator and platform is represented by the so-called *task space ellipsoid* at the end effector point or at the center of the object to be handled. The ellipsoid not only displays how a given task is contributed by the arm and the platform, but also the shape of the ellipsoid, kinematic or dynamic, naturally reflects constraint equations to which the platform is subjected.

The discussion in the paper is organized as follows. Section 2 describes the model of the mobile manipulator considered. Section 3 gives the derivations of the task space ellipsoid according to the model obtained in Section 2. Case study based on the derivations is presented in Section 4, followed by concluding remarks and future work.

2 Modeling of the System

In this section, we derive the motion equations of the two-arm mobile manipulator and the object, separately. Motion equations of the mobile manipulator which itself consists of multiple subsystems are obtained by adding dynamic interaction terms to pre-existing motion equations [15].

2.1 Motion Equation of the Mobile Manipulator

Like any other dynamic systems, a model of mobile manipulators provides a basis for the study of other issues including stability analysis, feedback control design, and computer simulations. Dynamic modeling of

0-7803-5180-0-5/99 $10.00 © 1999 IEEE

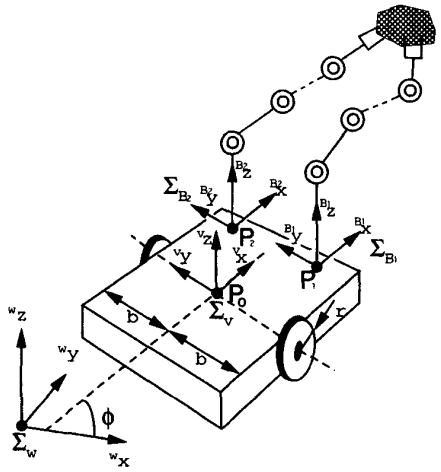

Figure 1: Wheeled mobile manipulator with two arms

mobile manipulators has been addressed by a number of researchers in the literature [5, 9, 4, 15].

In this paper, we consider two manipulators atop the mobile platform handling a common object as shown in Fig.1. Following a modular approach previously proposed [15], we derive the motion equations by fully utilizing the existing motion equations of the manipulators and of the mobile platform, and simply introducing additional terms that account for the dynamic interactions between the manipulators and the mobile platform.

$$ {}^1M\,{}^1\ddot{q} + {}^1C + {}^1G = {}^1\tau - {}^1R_v\,{}^v\ddot{q} - {}^1J^T h_1 \quad (1) $$

$$ {}^2M\,{}^2\ddot{q} + {}^2C + {}^2G = {}^2\tau - {}^2R_v\,{}^v\ddot{q} - {}^2J^T h_2 \quad (2) $$

$$ {}^vM\,{}^v\ddot{q} + {}^vC = E_v\,{}^v\tau - A^T\lambda_v - {}^vR_1\,{}^1\ddot{q} - {}^vR_2\,{}^2\ddot{q} \quad (3) $$

where Eq. (1) and (2) are the motion equations of the two individual manipulators while Eq. (3) represents the motion equation of the mobile platform.

Assuming that each arm has n degrees-of-freedom for the sake of convenience, the generalized coordinate vectors of the manipulators are given by[1]

$$ {}^1q = [{}^1q_1\ {}^1q_2 \cdots {}^1q_n]^T $$
$$ {}^2q = [{}^2q_1\ {}^2q_2 \cdots {}^2q_n]^T $$

In Eq. (1) and (2), ${}^iM$, ${}^iC$, and ${}^iG$ denote the $n \times n$ inertia matrix, n-dimensional velocity vector, and n-dimensional gravity vector of the manipulator i, respectively. It should be noted that although ${}^iM$ is solely determined by ${}^iq$, ${}^iC$ and ${}^iG$ in general are not. ${}^iC$ is affected by the velocity of the platform and ${}^iG$ is also influenced by platform's configuration if the platform moves around on a non-flat surface. ${}^i\tau$ is a n-dimensional input vector. ${}^iJ$ is Jacobian matrix. ${}^ih$ is the external force vector observed at the end-effector. ${}^iR_v$ is an $n \times m$ inertia matrix where m is the dimension of the generalized coordinates of the mobile platform, ${}^vq$, which will be stated shortly. ${}^iR_v$ is a function of ${}^iq$ and ${}^vq$. The last term of Eq. (1) and (2) represents the dynamic interaction caused by the motion of the mobile platform [15].

The mobile platform is subject to one holonomic constraint

$$ \phi = c(\theta_r - \theta_l) \quad (4) $$

and two nonholonomic constraints:

$$ \dot{x}_o \sin\phi - \dot{y}_o \cos\phi = 0 \quad (5) $$

$$ \dot{x}_o \cos\phi + \dot{y}_o \sin\phi = cb(\dot{\theta}_r + \dot{\theta}_l) \quad (6) $$

where (x_o, y_o) is the coordinates of point P_o in the inertia frame Σ_w, ϕ is the heading angle of the mobile robot measured from ${}^wX$-axis, θ_r and θ_l are the angular positions of the right wheel and the left wheel, respectively, and $c = \frac{r}{2b}$. The first nonholonomic constraint, Eq. (5), reflects the fact that no lateral slip is allowed between the wheels and the floor, while the second one, Eq. (6), corresponds to the no longitudinal slip constraint. Because of the holonomic constraint, ϕ may be easily eliminated from motion equations. Therefore, we choose the following generalized coordinate vector[2] :

$$ {}^vq = [x_o\ y_o\ \theta_r\ \theta_l]^T \quad (7) $$

With this generalized coordinate vector , the two nonholonomic constraints may be written as

$$ A({}^vq)\,{}^v\dot{q} = 0 \quad (8) $$

where

$$ A({}^vq) = \begin{bmatrix} -\sin\phi & \cos\phi & 0 & 0 \\ -\cos\phi & -\sin\phi & cb & cb \end{bmatrix} \quad (9) $$

In Eq. (3), ${}^vM$ and ${}^vC$ represent 4×4 inertia matrix and four-dimensional velocity vector. ${}^v\tau$ is a two-dimensional input vector which is the torque input for the two wheels. λ_v is a two-dimensional Lagrange multipliers corresponding to the nonholonomic constraints. ${}^vR_i$ is a $4 \times n$ inertia matrix which is a function of ${}^iq$ and ${}^vq$. The last two terms of Eq. (3) represent the dynamic interaction caused by the motion of the manipulators [15].

Next we reduce Eq. (3) by introducing a new set of unconstrained velocity coordinates in accordance with

[1] We use three kinds of superscript such as ${}^1q_2$, ${}^2C_1$ or ${}^vM$ throughout this paper. 1 and 2 correspond to the right-side manipulator and the left-side manipulator in Fig.1, respectively, while v refers to the mobile platform unless otherwise noted.

[2] m is actually 4 for the current choice of the platform coordinates.

the nonholonomic constraints. Let $S({}^v q)$ be a 4×2 matrix whose columns are in the null space of $A({}^v q)$ matrix in the constraint equation (8), *i.e.*, $A({}^v q)S({}^v q) = 0$. From the constraint equation (8), the velocity ${}^v\dot{q}$ must be in the null space of $A({}^v q)$. It follows that ${}^v\dot{q} \in span\{s_1({}^v q),\ s_2({}^v q)\}$, and that there exists a smooth vector $\eta = [\eta_1\ \eta_2]^T$ such that [13]

$$ {}^v\dot{q} = S({}^v q)\eta \tag{10} $$

and

$$ {}^v\ddot{q} = S({}^v q)\dot{\eta} + \dot{S}({}^v q)\eta \tag{11} $$

Using Eq. (10) and (11), and multiplying Eq. (3) by S^T, we have

$$ \begin{aligned} S^T({}^v M S\dot{\eta} + {}^v M\dot{S}\eta + {}^v C) = S^T E_v {}^v\tau \\ -S^T {}^v R_1 {}^1\ddot{q} - S^T {}^v R_2 {}^2\ddot{q} \end{aligned} \tag{12} $$

by noting that $S^T A^T = 0$.

Substituting Eq. (1) and (2) with Eq. (11), the motion equations of the manipulators become

$$ {}^1M {}^1\ddot{q} + {}^1C + {}^1G = {}^1\tau - {}^1R_v\dot{S}\eta - {}^1R_v S\dot{\eta} - {}^1J^T {}^1h \tag{13} $$

$$ {}^2M {}^2\ddot{q} + {}^2C + {}^2G = {}^2\tau - {}^2R_v\dot{S}\eta - {}^2R_v S\dot{\eta} - {}^2J^T {}^2h \tag{14} $$

Combining Eq. (12), (13), and (14), we obtain the following motion equations in matrix form:

$$ \begin{bmatrix} S^T {}^v MS & S^T {}^v R_1 & S^T {}^v R_1 \\ {}^1R_v S & {}^1M & 0 \\ {}^2R_v S & 0 & {}^2M \end{bmatrix} \begin{bmatrix} \dot{\eta} \\ {}^1\ddot{q} \\ {}^2\ddot{q} \end{bmatrix} = \begin{bmatrix} -S^T {}^v M\dot{S}\eta - S^T {}^v C \\ -{}^1C - {}^1G - {}^1R_v\dot{S}\eta \\ -{}^2C - {}^2G - {}^2R_v\dot{S}\eta \end{bmatrix} + \begin{bmatrix} S^T E_v & 0 & 0 \\ 0 & I & 0 \\ 0 & 0 & 1 \end{bmatrix} \begin{bmatrix} {}^v\tau \\ {}^1\tau \\ {}^2\tau \end{bmatrix} - J^T \begin{bmatrix} h_1 \\ h_2 \end{bmatrix} \tag{15} $$

or in more compact form,

$$ P\dot{x} = \xi + Q\tau - J^T h \tag{16} $$

where

$$ x = \begin{bmatrix} \eta \\ {}^1\dot{q} \\ {}^2\dot{q} \end{bmatrix} $$

$$ P = \begin{bmatrix} S^T {}^v MS & S^T {}^v R_1 & S^T {}^v R_1 \\ {}^1R_v S & {}^1M & 0 \\ {}^2R_v S & 0 & {}^2M \end{bmatrix} $$

$$ Q = \begin{bmatrix} S^T E_v & 0 & 0 \\ 0 & I & 0 \\ 0 & 0 & 1 \end{bmatrix} $$

$$ \xi = \begin{bmatrix} -S^T {}^v M\dot{S}\eta - S^T {}^v C \\ -{}^1C - {}^1G - {}^1R_v\dot{S}\eta \\ -{}^2C - {}^2G - {}^2R_v\dot{S}\eta \end{bmatrix} \quad \tau = \begin{bmatrix} {}^v\tau \\ {}^1\tau \\ {}^2\tau \end{bmatrix} $$

2.2 Motion Equation of the Object

Let h_o denote the m-dimensional vector of external forces applied at the center of mass of the object where m is the dimension of the task space. The force equation can be characterized as

$$ h_o = W\ h \tag{17} $$

where

$$ h = \begin{bmatrix} {}^1h \\ {}^2h \end{bmatrix} \tag{18} $$

The matrix W is a transformation matrix whose submatrices represent the force contributions of individual arms to the object. In the present two-arm case, W can be partitioned as

$$ W = [W_1\ \ W_2] \tag{19} $$

This matrix W attains a simple expression if described with respect to a coordinate frame fixed on the object [3]. It is noteworthy mentioning that, in that frame, for the case of rigid grasp or rolling contact, the matrix W becomes constant.

Based on the duality between forces and velocities that follows from the principle of virtual work, it can be shown that

$$ v = W^T\ v_o \tag{20} $$

where v_o is the m-dimensional vector of absolute velocities of the object, and $v = [{}^1v^T\ \ {}^2v^T]^T$ in which ${}^iv$ denotes absolute velocities of the end effector of i-th manipulator. Differentiating Eq. (20) with respect to time gives the acceleration equation in the form

$$ a = W^T\ a_o + \dot{W}^T\ v_o \tag{21} $$

where a_o is the m-dimensional vector of absolute object accelerations.

Motion equation of the object is given by [3]

$$ M_o a_o + c_o + g_o = h_o \tag{22} $$

where M_o is the $m \times m$ inertia matrix of the object, c_o and g_o are the m-dimensional vectors which represent velocity and gravity terms, respectively.

3 Task Space Ellipsoid

In this section, we derive the task space ellipsoid based on the motion equations obtained in the previous section. Kinematic ellipsoid is described first, followed by the derivation of dynamic ellipsoid.

3.1 Kinematic ellipsoid

Let $\dot{q}$ be the generalized velocity vector which is the same as x defined in the previous section[3] . In order

[3] Dimension of $\dot{q}$ is $2n + 2$ due to n for each manipulator and 2 for η.

to satisfy the implicit assumptions that the maximum velocities of all joints are the same and that the linear velocities and the angular velocities are of equal importance, we normalize $\dot{q}$ with the maximum joint velocities as follows.

$$\dot{\bar{q}} = Y\,\dot{q} \tag{23}$$

where

$$\begin{aligned} Y &= diag[Y_1\ Y_2\ \cdots\ Y_{2n+2}] \\ Y_i &= \frac{1}{\dot{q}_{i,max}} \qquad i = 1,\ \cdots\ 2n+2 \end{aligned}$$

If we set the desirable maximum velocity of the end-effector in the task space as unity in all directions, Jacobian matrix needs to be normalized as [18]

$$\hat{J} = J\,Y^{-1} \tag{24}$$

Now we consider a unit sphere in the joint space of the normalized joint velocities.

$$\dot{\bar{q}}^T\ \dot{\bar{q}} = 1 \tag{25}$$

Eq. (25) maps onto the ellipsoid in the object space of the absolute velocity as follows.

$$\begin{aligned} &(Y\hat{J}^{+}v)^T\ (Y\hat{J}^{+}v) \\ &\quad = (Y\hat{J}^{+}W^T v_o)^T\,(Y\hat{J}^{+}W^T v_o)^T \\ &\quad = {v_o}^T(Y\hat{J}^{+}W^T)^T\,(Y\hat{J}^{+}W^T)\ v_o \\ &\quad = 1 \end{aligned} \tag{26}$$

where $\hat{J}^{+}$ is Moore-Penrose pseudo inverse matrix which is represented by $\hat{J}^{+} = \hat{J}^T(\hat{J}\hat{J}^T)^{-1}$ when $\hat{J}$ is of full rank.

Eq. (26) yields the kinematic ellipsoid which takes into account both manipulation and locomotion of the mobile manipulator.

3.2 Dynamic ellipsoid

Next we consider the dynamics based on the motion equations obtained in the previous section.

If the mobile manipulator and the object are assumed to stand still ($\dot{q} = 0,\ v_o = 0$), it implies the following equations.

$$\begin{aligned} \eta = 0, \quad {}^1C = {}^2C = {}^vC = c_o = 0 \\ \dot{\hat{J}}\,\dot{q} = 0, \quad \dot{W}^T v_o = 0 \end{aligned}$$

From $a = J\ddot{q} + \dot{J}\dot{q}$ with the above assumptions,

$$a = J\,\ddot{q} \tag{27}$$

Also Eq. (16),(21) and (22), respectively, are simplified to:

$$\tau = Q^{-1}P\,\ddot{q} - Q^{-1}\xi + Q^{-1}J^T h \tag{28}$$

$$a = W^T a_o \tag{29}$$

$$M_o\,a_o + g_o = h_o \tag{30}$$

Eq. (27) and (29) yield

$$\ddot{q} = J^{+}W^T a_o \tag{31}$$

Combining Eq. (17) and (30),

$$W^{+}(M_o\,a_o + g_o) = h \tag{32}$$

Substituting Eq. (31) and (32) to (28), we obtain

$$\begin{aligned} \tau &= Q^{-1}P\,J^{+}W^T a_o - Q^{-1}\xi + \\ &\quad Q^{-1}J^T W^{+}(M_o\,a_o + g_o) \\ &= (Q^{-1}P\,J^{+}W^T + Q^{-1}J^T W^{+}M_o)\,a_o + \mu_o \\ &= \Lambda_o\,a_o + \mu_o \end{aligned} \tag{33}$$

where

$$\Lambda = Q^{-1}P\,J^{+}W^T + Q^{-1}J^T W^{+}M_o \tag{34}$$

$$\mu_o = Q^{-1}\xi + Q^{-1}J^T W^{+}\,g_o \tag{35}$$

Due to a similar reason to the one stated for the unit sphere in the joint velocity space, we normalize each element of the input torque vector τ by using the corresponding maximum torque input.

$$\bar{\tau} = Z\,\tau \tag{36}$$

where

$$\begin{aligned} Z &= diag[Z_1\ Z_2\ \cdots\ Z_{2n+2}] \\ Z_i &= \frac{1}{\tau_{i,max}} \qquad i = 1,\ \cdots\ 2n+2 \end{aligned}$$

The unit sphere in the joint space of the normalized torques

$$\bar{\tau}^T\ \bar{\tau} = 1 \tag{37}$$

maps onto the ellipsoid in the object space of the absolute accelerations

$$a_o^T\bar{\Lambda}_o^T\bar{\Lambda}_o a_o + 2a_o^T\bar{\Lambda}_o^T\bar{\mu}_o + \bar{\mu}_o^T\bar{\mu}_o = 1 \tag{38}$$

where $\bar{\Lambda}_o = Z\,\Lambda_o$ and $\bar{\mu}_o = Z\,\mu_o$. Eq. (38) yields the dynamic ellipsoid which takes into account contributions from both manipulation and locomotion of the mobile manipulator.

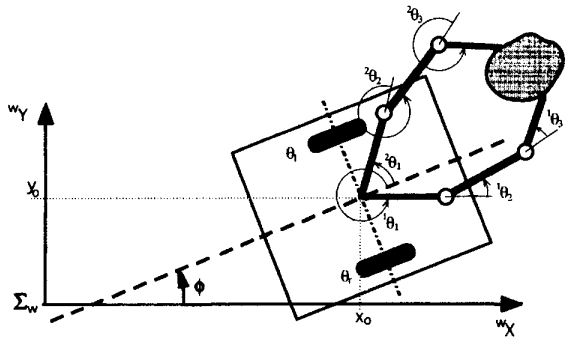

Figure 2: Schematic of a mobile manipulator with two arms used

Table 1: Parameters of manipulator

symbol (unit)	number of link or joint		
	first	second	third
L_i (m)	0.5	0.5	0.5
L_{ci} (m)	0.25	0.25	0.1
m_i (kg)	10	6	2
I_i (kgm^2)	0.5	0.3	0.01
$\tau_{i,max}$ (Nm)	200	100	30
$v_{i,max}$ (rad/s)	3.14	3.14	3.14

4 Case Study

Based on the derivations given in the previous section, we examine kinematic and dynamic ellipsoids for a particular example of two-arm mobile manipulators. Schematic of the system is shown in Figure 2. Each arm has three degrees-of-freedom and the both arms have the common origin at the midpoint between the wheels. All the assumptions made previously hold here. In addition, it is assumed that the motion of the system including the grasped object is horizontal. Therefore the effect of gravity is ignored.

4.1 Parameters used in case study

A set of parameters used in this case study is shown in Table 1 and 2^4 . where L_i is the length of the link, L_{ci} is the distance from the joint to the center of mass, m_i is the weight of the link, I_i is the moment of inertia of the link, $\tau_{i,max}$ is the maximum torque of the joint motor, and $v_{i,max}$ is the maximum velocity of the joint. Note that these parameters are common for the two manipulators. With the current choice of the system configuration, x $(= \dot{q})$ of Eq. (16) is given by

$$x = [\eta_1 \ \eta_2 \ {}^1\dot{\theta}_1 \ {}^1\dot{\theta}_2 \ {}^1\dot{\theta}_3 \ {}^2\dot{\theta}_1 \ {}^2\dot{\theta}_2 \ {}^2\dot{\theta}_3] \qquad (39)$$

[4] See [15] for the details of how these parameters are reflected in the motion equations.

Table 2: Parameters of mobile platform and object

symbol (unit)	value	description
b (m)	0.171	a half of the distance between the two driving wheels
r (m)	0.075	wheel radius
m_c (kg)	94.0	mass of the platform without the driving wheels and the rotors of the DC motors
m_w (kg)	5.0	mass of each driving wheel plus the rotor of its motor
I_c (kgm^2)	6.609	moment of inertia of the platform without the driving wheels and the rotors about a vertical axis through P_o
I_w (kgm^2)	0.01	moment of inertia of each wheel and the motor rotor about the wheel axis
I_m (kgm^2)	0.135	moment of inertia of each wheel and the motor rotor about the wheel diameter
$\tau_{i,max}$ (Nm)	200	maximum torque of each driving wheel
$v_{i,max}$ (rad/s)	$1/r$	maximum velocity of each driving wheel
m_o (kg)	2.0	mass of the object handled

4.2 Kinematic analysis

The initial configuration of the system is chosen such that the two arms hold the object in mirror symmetric configurations in which each arm achieves a globally optimal posture in terms of its own kinematic manipulability. Figure 3 shows how the shape of the ellipsoid at the end-effector is affected by the maximum velocities that the mobile platform can achieve. Three kinds of ellipsoids are presented for each configuration. For each case, the most inner ellipsoid in which the maximum velocity of the platform is kept very low is almost identical to that of a fixed dual arm system. Therefore the shape of the most inner ellipsoid is not affected by the relative configuration between the arms and the platform, because the platform can hardly move for this case. On the other hand, as the maximum velocity of the platform increases, the shape of the ellipsoid becomes more affected by the relative configuration. For instance, when the object is kept in front of the platform (0 deg.), the size of the ellipsoid will grow almost uniformly. This is because, with the object kept in front, the mobility of the platform can contribute the motion of the end-effector in all directions. However, if the object comes sideway (90 deg.), the platform can no longer contribute in the direction

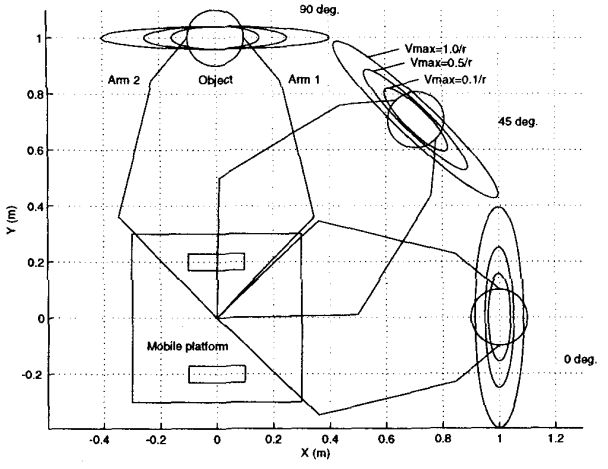

Figure 3: Kinematic ellipsoids with the different maximum velocities of the platform

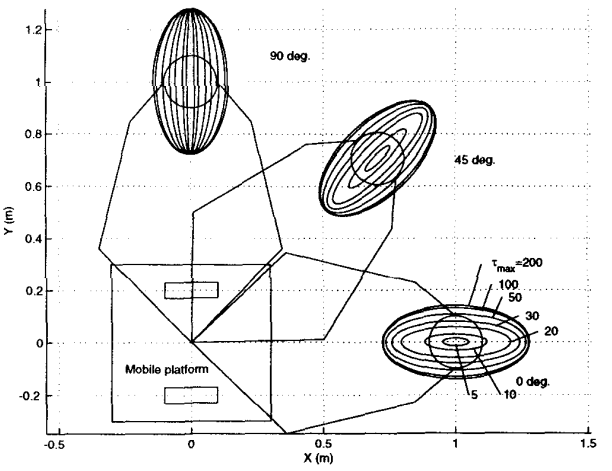

Figure 4: Dynamic ellipsoids with the different maximum torques of the platform

of minor axis due to the presence of nonholonomic constraints, although the platform still can contribute in other directions. Hence, this results in the unchanged minor axis in Figure 3.

4.3 Dynamic analysis

The same configurations as above are investigated from the dynamics point of view according to Eq. (38). If the motion of the system is confined in horizontal surface, then the gravitational term can be omitted

$$\mu_o = 0. \tag{40}$$

Therefore, under the assumptions, Eq. (38) is simplified to

$$a_o^T \overline{\Lambda}_o^T \overline{\Lambda}_o a_o = 1 \tag{41}$$

We also neglect dynamic interaction forces between the manipulators and the platform for simplicity reason.

Figure 4 shows the dynamic ellipsoids with varying maximum input torques of the driving wheels. The outer most ellipsoids remain the same regardless of the relative configurations between the manipulators and the platform because, with the large input torque of the driving wheels (τ_{max}=200), the system almost behaves like a fixed dual-arm system. However, as the input torque decreases, the ellipsoid will rapidly shrink and also be affected by the location of the object relative to the platform. If the object is located in front of the platform, the size of the ellipsoid becomes smaller almost uniformly as the maximum torque decreases. On the other hand, when the object comes sideway, the major axis of the ellipsoid remains unchanged due to the nonholonomic constraints.

5 Conclusion

In this paper, we introduced a task space ellipsoid for mobile manipulators. This ellipsoid represents how the manipulator and the platform can contribute to a given task at the end effector kinematically or dynamically. We also showed through a case study that the shape of the ellipsoid, kinematic or dynamic, naturally reflects constraint equations to which the platform is subjected.

Future work will be to investigate how to apply the proposed ellipsoid in order to synthesize individual motions of the manipulator and the platform, and to extend to similar, but different problems such as coordination of multiple mobile manipulators.

References

[1] W. F. Carriker, P. K. Khosla, and B. H. Krogh. Path planning for mobile manipulators for multiple task execution. *IEEE Transactions on Robotics and Automation*, 7(3):403–408, June 1991.

[2] P. Chiacchio, S. Chiaverini, L. Sciavicco, and B. Siciliano. On the manipulability of dual cooperative robots. In *Proceedings of NASA Conference on Space Telerobotics Conference*, pages 351–360, Pasadena, CA, January 1989.

[3] P. Chiacchio, S. Chiaverini, L. Sciavicco, and B. Siciliano. Task space dynamic analysis of multiarm system configurations. *The International Journal of Robotics Research*, 10(6):708–715, 1991.

[4] S. Dubowsky and A. B. Tanner. A study of the dynamics and control of mobile manipulators subjected to vehicle disturbances. In *Proceedings of 4th International Symposium of Robotics Research*, pages 111–117, Santa Cruz, CA, August 1987.

[5] N. A. M. Hootsmans. *The Motion Control of Manipulators on Mobile Vehicles.* PhD thesis, Department of Mechanical Engineering, Massachusetts Institute of Technology, Cambridge, MA, January 1992.

[6] C. A. Klein and B. E. Blaho. Dexterity measures for the design and control of kinematically redundant manipulators. *The International Journal of Robotics Research*, 6(2):72–83, 1987.

[7] S. Lee. Dual redundant arm configuration optimization with task-oriented dual arm manipulability. *IEEE Transactions on Robotics and Automation*, 5(1):78–97, 1989.

[8] Z. Li, P. Hsu, and S. Sastry. Grasping and coordinated manipulation by a multifingered hand. *The International Journal of Robotics Research*, 8(4):33–50, 1989.

[9] K. Liu and F. L. Lewis. Decentralized continuous robust controller for mobile robots. In *Proceedings of 1990 International Conference on Robotics and Automation*, pages 1822–1827, Cincinnati, OH, May 1990.

[10] W. Miksch and D. Schroeder. Performance-functional based controller design for a mobile manipulator. In *Proceedings of 1992 International Conference on Robotics and Automation*, pages 227–232, Nice, France, May 1992.

[11] F. G. Pin and J. C. Culioli. Optimal positioning of combined mobile platform-manipulator systems for material handling tasks. *Journal of Intelligent and Robotic Systems*, 6:165–182, 1992.

[12] H. Seraji. An on-line approach to coordinated mobility and manipulation. In *Proceedings of 1993 International Conference on Robotics and Automation*, pages 28–35, Vol. 1, Atlanta, GA, May 1993.

[13] Y. Yamamoto and X. Yun. Coordinating locomotion and manipulation of a mobile manipulator. *IEEE Transactions on Automatic Control*, 39(6):1326–1332, June 1994.

[14] Y. Yamamoto and X. Yun. Coordinated obstacle avoidance of a mobile manipulator. In *Proceedings of 1995 International Conference on Robotics and Automation*, pages 2255–2260, Nagoya, Japan, May 1995.

[15] Y. Yamamoto and X. Yun. A modular approach to dynamic modeling of a class of mobile manipulators. *International Journal of Robotics and Automation*, 12(2):41–48, 1997.

[16] T. Yoshikawa. Dynamic manipulability of robot manipulators. *Journal of Robotic Systems*, 2(2):113–124, 1985.

[17] T. Yoshikawa. Manipulability of robotic mechanisms. *The International Journal of Robotics Research*, 4(1):3–9, 1985.

[18] T. Yoshikawa. *Foundations of Robotics: Analysis and Control.* The MIT Press, Cambridge, MA, 1990.